Proposed realization of itinerant ferromagnetism in optical lattices

Shizhong Zhang,[1,2] Hsiang-hsuan Hung,[3] and Congjun Wu[3]
[1]*Department of Physics, University of Illinois at Urbana-Champaign, Urbana, Illinois 61801, USA*
[2]*Department of Physics, Ohio State University, Columbus, Ohio 43210, USA*
[3]*Department of Physics, University of California, San Diego, California 92093, USA*
(Received 24 March 2010; revised manuscript received 2 October 2010; published 17 November 2010)

We propose a scheme to realize the itinerant ferromagnetism of two-component cold fermionic atoms in the p-orbital bands in optical lattices. The band flatness in the two-dimensional honeycomb lattice dramatically amplifies the interaction effect, driving the ferromagnetic transition even with a relatively weak repulsive interaction. This scheme has the advantage that the stability of the system can be maintained without causing decay to the molecular state as one approaches the Feshbach resonance from the side with the positive scattering length. Experimental signatures and detections are also discussed.

DOI: 10.1103/PhysRevA.82.053618 PACS number(s): 03.75.Ss, 03.75.Mn, 71.10.Fd, 05.50.+q

I. INTRODUCTION

Itinerant ferromagnetism (FM) is one of the central topics in condensed-matter physics [1–7], and its mechanism remains a controversial problem. The major difficulty is that FM does not have a well-defined weak-coupling picture, that is, spontaneous spin polarization requires interactions strong enough to overcome the kinetic-energy cost. Furthermore, unlike most superconductors in which fermionic excitations are gapped except at nodal points that have zero measure, ferromagnets have completely gapless Fermi surfaces. The gapless particle-hole excitations dramatically complicate the nature of the transition. Important progress in understanding FM has been made by Mielke [8] and Tasaki [9], who provide a class of exactly solvable models with FM ground states. The key point is the existence of Wannier-like orbitals for single-particle eigenstates, which reduce the kinetic-energy cost of spin polarization to zero. However, these models must operate under the stringent conditions of fine-tuned long-range hopping, which is difficult to realize.

In spite of its importance, itinerant FM has not been realized in cold-atom systems, partly because of the requirement of the previously mentioned strong repulsion. It has been proposed [10] that FM can be achieved by approaching the Feshbach resonance from the side with the positive scattering length. However, a problem is that before the interaction is strong enough to drive the transition, the system is unstable toward to the formation of the dimer-molecules [11].

On the other hand, orbital physics in optical lattices has received a great deal of attention, which has given rise to a variety of new states of matter with both cold bosons and fermions [12–21]. In particular, it was shown recently that the p-orbital band in the honeycomb lattice, a p_x (p_y)-orbital counterpart of graphene, has a natural excellent flat-band structure. The consequential nonperturbative interaction effects (e.g., Wigner crystallization) associated with the band flatness have been investigated [15,16]. Experimentally, the honeycomb lattice was constructed quite some time ago [22].

In this paper, we propose a scheme to realize the ferromagnetic state in the p-orbital band of the honeycomb optical lattice by taking advantage of its band flatness. Due to the divergence of the density of states, even weak repulsions can drive the ferromagnetic transition. This ensures the system's stability during the formation of dimer molecules, thus overcoming the experimental difficulty mentioned earlier. We show the existence of the exact ferromagnetic ground state at the filling level $0.25 < \langle n \rangle < 0.5$, and we investigate the phase boundaries between ferromagnetic, paramagnetic, and antiferromagnetic states through the self-consistent mean-field method. This research will open up opportunities to investigate FM with precise controllability.

II. FLAT-BAND FERROMAGNETISM

We begin with the free part of the p_x (p_y)-orbital band Hamiltonian in the honeycomb lattice,

$$H_0 = t_{\parallel} \sum_{\vec{r}\in A,i,\sigma} (p^{\dagger}_{\vec{r},i,\sigma} p_{\vec{r}+a\hat{e}_i,i,\sigma} + \text{H.c.}) - \mu \sum_{\vec{r}\sigma} n_{\vec{r}\sigma}, \qquad (1)$$

where $\hat{e}_{1,2} = \pm\frac{\sqrt{3}}{2}\hat{e}_x + \frac{1}{2}\hat{e}_y$ and $\hat{e}_3 = -\hat{e}_y$ are the unit vectors pointing from an A site to its three B-site neighbors, $p_i \equiv (p_x\hat{e}_x + p_y\hat{e}_y)\hat{e}_i$ ($i = 1 \sim 3$) are the projections of the p orbitals along the $\hat{e}_i$ direction, $n_{\vec{r},\sigma}$ is the number operator for spin σ, and μ is the chemical potential. As illustrated in Refs. [15,16], its band structure contains both flat bands and Dirac cones whose spectra are symmetric with respect to the zero energy. Two dispersive bands in the middle have two nonequivalent Dirac points with a bandwidth of $\frac{3}{2}t_{\parallel}$. The bottom and top bands turn out to be completely flat in the absence of the π-bonding $t_{\perp}$, which means that the single-particle eigenstates of Eq. (1) can be constructed as a set of degenerate *localized* states. There exists one such eigenstate in the bottom band for each hexagon plaquette, whose orbital configuration on each site is along the tangential direction around the plaquette. The anisotropy of the σ bonding and the destructive interference together prevent the particle from "leaking" outside, which renders these states eigenstates.

The interaction of the spinful neutral fermions is described within the s-wave scattering approximation, leading to a

two-band Hubbard model constructed as

$$H_{\rm int} = U\sum_{\vec{r}}(n_{\vec{r},x\uparrow}n_{\vec{r},x\downarrow} + n_{\vec{r},y\uparrow}n_{\vec{r},y\downarrow}) - J\sum_{\vec{r}}\left(\vec{S}_{\vec{r}x}\cdot\vec{S}_{\vec{r}y} - \frac{1}{4}n_{\vec{r}x}n_{\vec{r}y}\right) + \Delta(p^{\dagger}_{\vec{r}x\uparrow}p^{\dagger}_{\vec{r}x\downarrow}p_{\vec{r}y\downarrow}p_{\vec{r}y\uparrow} + \text{H.c.}), \quad (2)$$

where $U = \frac{4\pi\hbar^2}{m}a_s\int|p_x(\vec{r})|^4d^3\vec{r}$ (a_s is the scattering length), $J = \frac{2U}{3}$, $\Delta = \frac{U}{3}$, $\vec{S}_{\vec{r}x} = \frac{\hbar}{2}p^{\dagger}_{\vec{r}x\alpha}\vec{\sigma}_{\alpha\beta}p_{\vec{r}x\beta}$ is the spin operator at site $\vec{r}$ in the p_x orbital, and $\vec{S}_{\vec{r}y}$ can be defined accordingly. The U term is just the usual Hubbard term; the J term represents Hund's rule physics: the on-site repulsion between two fermions in the spin-triplet states is zero, while that of the spin singlet is J; the Δ term describes the pair scattering process between the p_x and p_y orbitals on the same site. We first consider two fermions on the same site to gain some intuition. If they are in the spin-triplet channel, their orbital wave function is antisymmetric, thus the s-wave interaction vanishes. If they are in the spin-singlet channel, their orbital wave functions are symmetric as $p_x^2 + p_y^2$, $p_x^2 - p_y^2$, and p_xp_y, respectively. The first one has energy $U + \Delta = \frac{4U}{3}$, while the latter two are degenerate with energy $U - \Delta = J = \frac{2U}{3}$.

At low filling factors, $\langle n\rangle \leqslant \frac{1}{2}$, the ground states are heavily degenerate. Each fermion occupies one localized plaquette state. The touching of two neighboring plaquettes with the same spin costs zero repulsion energy, while that of the opposite spin costs an energy of $\frac{U}{36}$. According to the percolation picture of the flat-band FM [8,9], fermions form disconnected clusters composed of touching plaquettes. Let us denote the total number of sites as N. There are then $\frac{N}{2}$ plaquettes whose centers form a triangular lattice. These clusters are labeled from 1 to n_c. The number of plaquettes inside the ith cluster is denoted as m_i ($i = 1 \sim n_c$). Thus the particle density is just $\langle n\rangle = \sum_{i=1}^{n_c} m_i/N$. Within each cluster, the fermions are fully polarized but the polarizations of different clusters are uncorrelated. The ferromagnetic order parameter when $\langle n\rangle \leqslant \frac{1}{2}$ is defined as $M = \sqrt{\langle S^2_{z,\rm tot}\rangle}/N$, where the square of total spin of the system is just $S^2_{z,\rm tot} = (\frac{\hbar}{2})^2\sum_{i=1}^{n_c} m_i^2$, and $\langle\rangle$ denotes the average over all possible configurations of the degenerate ground states. As the filling increases beyond the percolation threshold, clusters become connected driving the system from a paramagnetic state to a ferromagnetic state. We have performed numeric simulations and obtained M versus $\langle n\rangle$ as depicted in Fig. 1. M becomes nonzero approximately beyond the percolation threshold $n_c = 0.25$ (the small deviation is due to the finite-size effect), which corresponds to the site-percolation threshold $p_c = 0.5$ for the triangular lattice. As we go beyond the percolation threshold, there is a unique infinite cluster with nonzero probability in the triangular lattice [23], thus M is just the probability of a site belonging to the infinite cluster and behaves as $M \propto (\langle n\rangle - n_c)^{\beta}$, with the critical exponent $\beta = \frac{5}{32}$ [23]. As $\langle n\rangle$ increases further, M is linear with $\langle n\rangle$, which means that the system is almost fully polarized.

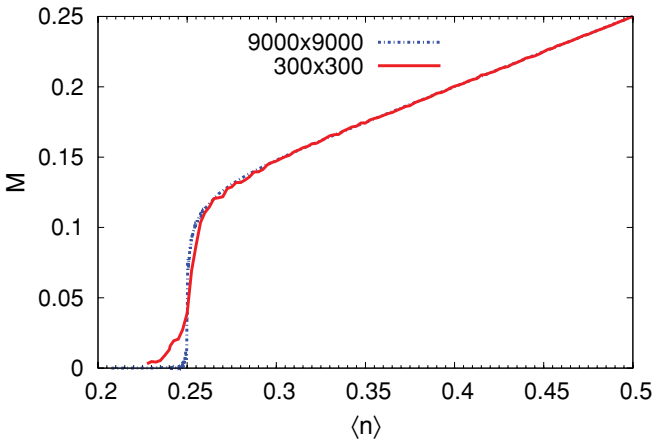

FIG. 1. (Color online) The magnetization M vs $\langle n\rangle$ for $0 < \langle n\rangle < \frac{1}{2}$ simulated on a triangular lattice with 9000×9000 lattice sites (blue line) and 300×300 lattice sites (red line). Note the strong finite-size effect around the percolation threshold $\langle n\rangle_c = 1/4$.

III. MEAN-FIELD THEORY IN THE HOMOGENEOUS SYSTEM

After the lowest flat band is fulfilled with spin-polarized fermions, that is, $\langle n\rangle > \frac{1}{2}$, an exact solution is no longer available. We perform a self-consistent mean-field calculation. To facilitate the decomposition of the interaction term of Eq. (2), we can recast it in an equivalent form $H_{\rm int} = \sum_{\vec{r}}\frac{8U}{3}I_{\vec{r}\uparrow}I_{\vec{r}\downarrow} + \sum_{\vec{r}}\frac{4U}{3}(\tau^{(1)}_{\vec{r}\uparrow}\tau^{(1)}_{\vec{r}\downarrow} + \tau^{(2)}_{\vec{r}\uparrow}\tau^{(2)}_{\vec{r}\downarrow})$, where the pseudo-spin-operators $\tau^{(1,2)}_{\uparrow,\downarrow}$ are defined as $\tau^{(1)}_{\uparrow,\downarrow} = \frac{1}{2}(p^{\dagger}_{x\uparrow,\downarrow}p_{y\uparrow,\downarrow} + p^{\dagger}_{y\uparrow,\downarrow}p_{x\uparrow,\downarrow}), \tau^{(2)}_{\uparrow,\downarrow} = \frac{1}{2}(p^{\dagger}_{x\uparrow,\downarrow}p_{x\uparrow,\downarrow} - p^{\dagger}_{y\uparrow,\downarrow}p_{y\uparrow,\downarrow})$, and $I_{\uparrow,\downarrow} = \frac{1}{2}(p^{\dagger}_{x\uparrow,\downarrow}p_{x\uparrow,\downarrow} + p^{\dagger}_{y\uparrow,\downarrow}p_{y\uparrow,\downarrow})$, respectively. Here $\tau^{1,2}$ measures the preferential occupation of x and y orbitals, and I is half of the identity operator in the p_x and p_y orbitals. Although this does not make the spin SU(2) symmetry explicit, it is convenient for the mean-field decoupling if the spin-quantization axis is chosen along the z direction. The mean-field Hamiltonian then reads, apart from a constant part,

$$H^{\rm mf}_{\rm int} = \sum_{\vec{r}}\frac{8U}{3}\{I_{\vec{r}\uparrow}\langle I_{\vec{r}\downarrow}\rangle + \langle I_{\vec{r}\uparrow}\rangle I_{\vec{r}\downarrow}\} + \sum_{\vec{r}}\frac{4U}{3}\{\langle\tau^{(1)}_{\vec{r}\uparrow}\rangle\tau^{(1)}_{\vec{r}\downarrow} + \tau^{(1)}_{\vec{r}\uparrow}\langle\tau^{(1)}_{\vec{r}\downarrow}\rangle + \langle\tau^{(2)}_{\vec{r}\uparrow}\rangle\tau^{(2)}_{\vec{r}\downarrow} + \tau^{(2)}_{\vec{r}\uparrow}\langle\tau^{(2)}_{\vec{r}\downarrow}\rangle\}. \quad (3)$$

The ferromagnetic order parameter is defined as $M = \sum_{\vec{r}}(I_\uparrow - I_\downarrow)/N$. We enlarge the unit cell to include six lattice sites to allow site-dependent magnetic and orbital configurations. We also replace the bare value of U with an effective one in the self-consistent calculation by taking into account the Kanamori corrections defined as $U_{\rm eff}(\mu) = U(\vec{p},\vec{q};\mu)$ at $p,q \to 0$ [24,25]. $U(\vec{p},\vec{q};\mu)$ is defined as $U(\vec{p},\vec{q};\mu) = U/[1 - U\Pi(\vec{p},\vec{q})]$, and

$$\Pi = 1/N\sum_{\vec{k}}{}'[E(\vec{q}) + E(\vec{p}) - E(\vec{k}) - E(\vec{p} + \vec{q} - \vec{k})], \quad (4)$$

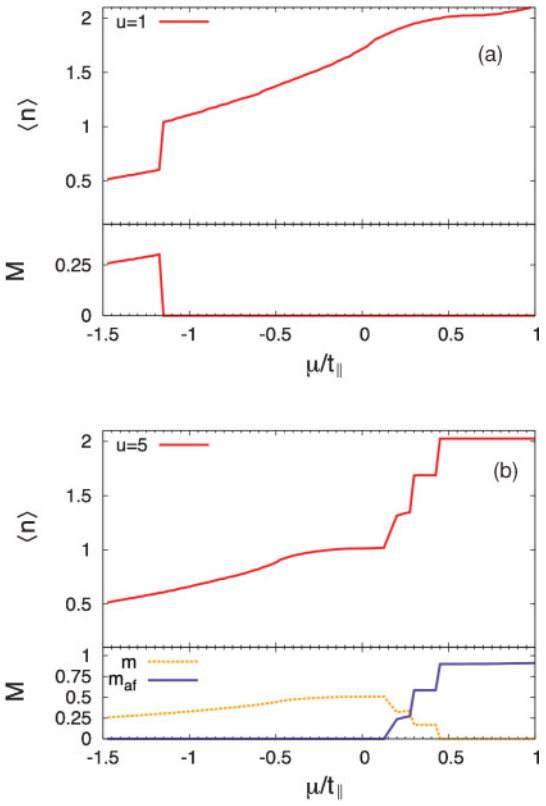

FIG. 2. (Color online) (a) Filling factor n and magnetization m vs the chemical potential μ at weak interaction ($U/t_\parallel = 1$). (b) n, m, and antiferromagnetic moment $m_{\rm af}$ vs μ at strong interaction ($U/t_\parallel = 5$).

where $E(\vec{k})$ is the band energy corresponding to Eq. (1), and the summation over $\vec{k}$ is taken over unoccupied Bloch states. The renormalization procedure ensures that $U_{\rm eff}$ can be of the same order as the bandwidth at most and thus precludes FM in the usual Hubbard model at low density even for very large bare U [25].

As $\langle n\rangle$ increases beyond $\frac{1}{2}$, the flat band is fulfilled with polarized particles with $\mu/t_\parallel > -1.5$. The additional particles have to either flip their spin and fill the flat-band states, costing energy of order U, or continue to fill the second band while remaining spin-polarized. The competition between the kinetic energy and the interaction energy determines a critical chemical potential μ_c as a function of U, beyond which the full polarization is no longer favorable. Within the mean-field theory, we compare the energies of fully polarized ferromagnetic states $E_{\rm ferro}(U,\mu)$ and that of a paramagnetic state $E_{\rm para}(U,\mu)$, and then determine μ_c. As depicted in Fig. 2(a), we show the dependence of $\langle n\rangle$ and M as a function of μ at a weak coupling $U/t_\parallel = 1$. Note that $\langle n\rangle$ and m both jump at $\mu_c \approx -1.15$, which is a consequence of the flat-band structure. When the minority spins begin to populate, the divergent density of states of the flat band suddenly increases its filling, which significantly changes the effective potential that the majority spins feel and drives the system to paramagnetic states. In other words, if the particle density is fixed between the two values before and after the jump, we obtain the phase-separation state as the coexistence of the fully polarized state and the paramagnetic state. After the paramagnetic phase is reached, the system remains in a metallic state at small U because of the vanishing of the density of states of the Dirac cone at half-filling.

The phase diagram becomes richer as U becomes stronger, as depicted in Fig. 2(b) with $U/t_\parallel = 5$. The fully polarized state survives to a larger $\mu_c/t_\parallel \approx 0.1$ as expected; the Mott-insulating antiferromagnetic state occurs at half-filling $\langle n\rangle = 2$ with the Néel order defined as $M_{\rm af} = \frac{1}{N}\sum_i (-)^i S_z^i$. In the strong-coupling limit at half-filling, each site is filled with two particles and spin-aligned by Hund's rule as a spin-1 complex. The virtual hopping of particles leads to the antiferromagnetic exchange and the long-range Néel order in the ground state. At intermediate fillings between the fully polarized state and the antiferromagnetic state, as $\mu > \mu_c$, the quick increase of $\langle n\rangle$ is due to the filling of the minority spins in the flat band. Interestingly, an incompressible state occurs at $\langle n\rangle = 5/3$ with $\langle n_\uparrow\rangle = 1$ and $\langle n_\downarrow\rangle = 2/3$, which has the coexistence of the partial ferromagnetic and antiferromagnetic orders, that is, the ferrimagnetic order. It also exhibits an intricate orbital ordering pattern as in the spinless case [15,16]. We defer a detailed analysis of this state to a future publication.

Now we discuss the effect of the small π-hopping term $t_\perp$. Then the lowest-energy band acquires a weak dispersion with a bandwidth of order $t_\perp$. In this case, the localized plaquette states are no longer eigenstates of the system. However, as long as the interaction strength U is much larger than $t_\perp$, it is not energetically favorable to flip the spin, and thus the ferromagnetic state is stable. As shown in Ref. [16], in realistic systems with the sinusoidal optical potential, it is easy to suppress $t_\perp/t_\parallel$ to 10^{-2} or even 10^{-3}. We have confirmed the existence of ferromagnetic order numerically by using the previously mentioned mean-field theory for $t_\perp$ up to $0.1t_\parallel$.

Another small interaction which was previously left out is the p-wave scattering U'. It adds an extra interaction term $\Delta H_{\rm int} = \sum_{\vec{r}} U' n_{\vec{r}x} n_{\vec{r}y}$, and the value of J in Eq. (2) changes to $J' = \frac{2}{3}U - U'$. In this case, the flat-band structure is not destroyed, but an exact solution is no longer available as long as $\langle n\rangle > 1/6$ because different plaquettes touch and cost energy of order U' even with polarized spin. We have also performed self-consistent mean-field theory to check that the ferromagnetic state is still stable at a small value of U'. For example, for the case of $U/t_\parallel = 5, U'/t_\parallel = 1$, we find that the ferromagnetic order survives up to a filling factor $\langle n\rangle \approx 1$.

Now we discuss the finite-temperature effect. We only consider the case of the filled flat band whose low-energy excitations are captured by an effective ferromagnetic Heisenberg model defined for plaquette spins [8], and we leave the study of the general filling to a future publication. In our case, the effective model is constructed on a triangular lattice as $H_{\rm ex} = -J'\sum \vec{S}_i \cdot \vec{S}_j$ with $J' \approx \frac{U}{18}$. The mean-field calculation based on Eq. (2) shows that the critical temperature $T_{\rm mf}$ is at the same order of $zJ'/2$ for small values of $U/t_\parallel$ at $\langle n\rangle = \frac{1}{2}$, where $z = 6$ is the coordination number. $T_{\rm mf}$ is the temperature scale for the onset of the nonzero magnitude of the ferromagnetic order parameter, which is roughly one order smaller than U. According to the data in Ref. [26], $T_{\rm mf}$ can be estimated as the order of 1–10 nK, which remains experimentally accessible. Below $T_{\rm mf}$, thermal fluctuations of the orientation of the ferromagnetic order are described by the O(3) nonlinear-σ model, and no true long-range order exists

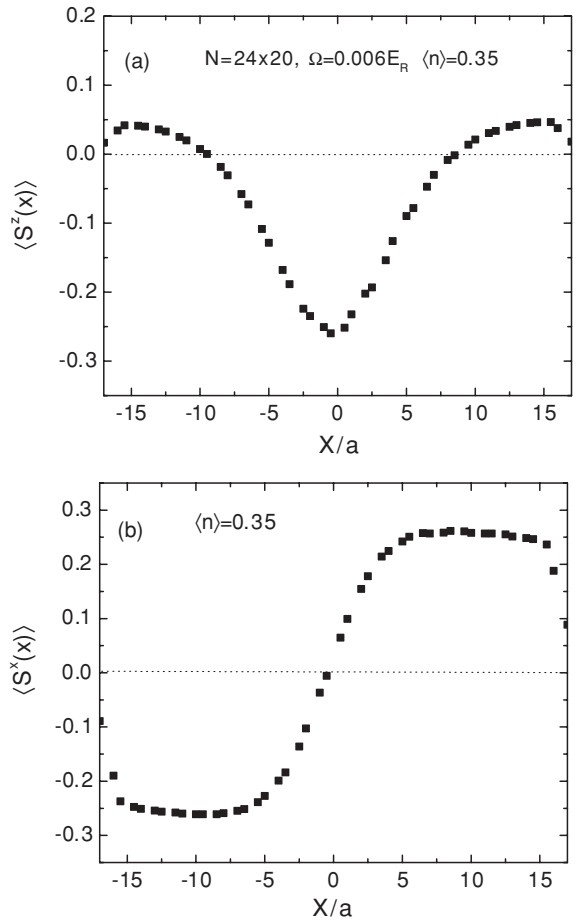

FIG. 3. The skyrmion configuration of the spin-density distribution in the confining trap with parameters $U/E_R = 1$, $t_\perp/E_R = 0.24$, $\Omega/E_R = 0.006$, and $n_\uparrow = n_\downarrow = 168$. The total number of unit cells is $N = 24 \times 20$ (the number of sites is $2N$). (a) $\langle S_z(\vec{r})\rangle$ along the line of $(X/a, Y/a = 0)$, that is, the center row in the system. (b) $\langle S_x(\vec{r})\rangle$ pattern along the line of $(X/a, Y/a = 0)$. $\langle S_y(\vec{r})\rangle$ shows a similar behavior along $(X/a = 0, Y/a)$.

for $T > 0$ in two dimensions. However, the spin-correlation length ξ diverges fast as $\xi/a \approx e^{T_{\rm mf}/T}$ (a is the lattice constant), which can easily exceed the small size of the optical lattice (e.g., typically $L/a \approx 50$) as T becomes smaller than $T_{\rm mf}$. Thus practically we can still take $T_{\rm mf}$ as the onset temperature scale of ferromagnetism.

IV. EFFECTS FROM THE CONFINING TRAPPING POTENTIAL

Next we study the effect of the overall harmonic trapping potential $V_{\rm tr}(\vec{r}) = \frac{m}{2}\Omega^2 r^2$ and show that FM remains robust through a self-consistent Bogoliubov–de Gennes calculation in real space. In experiments, the particle number of each component is conserved separately. Furthermore, when the system has SU(2) symmetry as in Eq. (2), the spin configuration prefers the skyrmion configuration rather than the Ising domain wall [27] to lower the energy. The skyrmion-type real-space magnetization distributions of $\langle S_z(\vec{r})\rangle$ and $\langle S_x(\vec{r})\rangle$ are depicted in Figs. 3(a) and 3(b), respectively, with the parameters $U/t_\parallel = 1$, $\Omega = 0.006E_R$ (E_R is the recoil energy), and $t_\parallel/E_R = 0.24$ as calculated in Ref. [16]. The characteristic trap length scale is $l = \sqrt{\frac{\hbar}{m\Omega}} \approx 4.1a$, where a is the lattice constant. We take particle numbers of spin-$\uparrow$ and spin-$\downarrow$ components as $n_\uparrow = n_\downarrow = 168$, which can be achieved by introducing two different chemical potentials for $\mu_\uparrow = -1.3897$ and $\mu_\downarrow = -1.3903$. The spin-$\downarrow$ particles concentrate in the center region, whereas most spin-$\uparrow$ particles live outside and form a ring. The spin distribution varies smoothly from $\downarrow$ to $\uparrow$ from the central region to the outside due to the spin SU(2) symmetry. Experimentally, the shell structure can be resolved *in situ* by the tomographic radiofrequency spectroscopic method [28] followed by a phase-contrast imaging technique [29] which can distinguish the shell structures with two different components.

V. CONCLUSIONS

In summary, we have proposed a scheme to realize itinerant FM by using the flat-band structure in the p-orbital system in the honeycomb lattice. The band flatness stabilizes FM even with weak repulsive interactions, thus the stability problem of using Feshbach-type methods is avoided. The FM is robust against soft trapping potentials, exhibiting the skyrmion-type configuration as a result of spin conservation. Furthermore, due to the large configuration space of the partially filled flat band, flat-band FM supports large entropy, which makes this proposal even more realistic. This work provides a potential way to realize spin transport and even spintronics in future research with cold atoms.

Note added in proof. Recently, we learned of independent works by Wang *et al.* [30] and Berdnikov *et al.* [27] on FM with cold atoms. Evidence of FM has been observed in a recent experiment through Feshbach resonances by Jo *et al.* [31].

ACKNOWLEDGMENTS

S.Z. is supported by NSF-DMR-03-50842. C.W. thanks J. Hirsch and L. Sham for helpful discussions. C.W. and H.H.H. are supported by the Sloan Research Foundation, ARO-W911NF0810291, and NSF-DMR-0804775.

[1] J. A. Hertz, Phys. Rev. B **14**, 1165 (1976).
[2] A. J. Millis, Phys. Rev. B **48**, 7183 (1993).
[3] D. Belitz *et al.*, Rev. Mod. Phys. **77**, 579 (2005).
[4] H. v Löhneysen *et al.*, Rev. Mod. Phys. **79**, 1015 (2007).
[5] J. E. Hirsch, Phys. Rev. B **40**, 2354 (1989).
[6] T. Moriya, *Spin Fluctuations in Itinerant Electron Magnets* (Springer, Berlin, 1975).
[7] D. C. Mattis, *The Theory of Magnetism I* (Springer-Verlag, Berlin, 1981).
[8] A. Mielke *et al.*, Commun. Math. Phys. **158**, 341 (1993).

[9] H. Tasaki, Phys. Rev. Lett. **75**, 4678 (1995).
[10] R. A. Duine and A. H. MacDonald, Phys. Rev. Lett. **95**, 230403 (2005).
[11] T. L. Ho and E. J. Mueller, Phys. Rev. Lett. **92**, 160404 (2004).
[12] A. Isacsson and S. M. Girvin, Phys. Rev. A **72**, 053604 (2005).
[13] W. V. Liu and C. Wu, Phys. Rev. A **74**, 013607 (2006).
[14] A. B. Kuklov, Phys. Rev. Lett. **97**, 110405 (2006).
[15] C. Wu, D. Bergman, L. Balents, and S. Das Sarma, Phys. Rev. Lett. **99**, 070401 (2007).
[16] C. Wu and S. Das Sarma, Phys. Rev. B **77**, 235107 (2008).
[17] V. Stojanovic, C. Wu, W. V. Liu, and S. Das Sarma, Phys. Rev. Lett. **101**, 125301 (2008).
[18] C. Xu and M. P. A. Fisher, Phys. Rev. B **75**, 104428 (2007).
[19] K. Wu and H. Zhai, Phys. Rev. B **77**, 174431 (2008).
[20] T. Mueller, S. Folling, A. Widera, and I. Bloch, Phys. Rev. Lett. **99**, 200405 (2007).
[21] J. Sebby-Strabley, M. Anderlini, P. S. Jessen, and J. V. Porto, Phys. Rev. A **73**, 033605 (2006).
[22] G. Grynberg, B. Lounis, P. Verkerk, J. Y. Courtois, and C. Salomon, Phys. Rev. Lett. **70**, 2249 (1993).
[23] S. Strauffer and A. Aharony, *Introduction to Percolation Theory*, 2nd rev. ed. (Taylor&Francis, London, 1994).
[24] J. Callaway, *Quantum Theory of the Solid State* (Academic, New York, 1974).
[25] P. Fazekas, *Lecture Notes on Electron Correlation and Magnetism* (World Scientific, Singapore, 1999).
[26] T. L. Ho and Q. Zhou, Phys. Rev. Lett. **99**, 120404 (2007).
[27] I. Berdnikov, P. Coleman, and S. H. Simon, Phys. Rev. B **79**, 224403 (2009).
[28] Y. Shin, C. H. Schunck, A. Schirotzek, and W. Ketterle, Phys. Rev. Lett. **99**, 090403 (2007).
[29] Y. Shin, M. W. Zwierlein, C. H. Schunck, A. Schirotzek, and W. Ketterle, Phys. Rev. Lett. **97**, 030401 (2006).
[30] L. Wang, X. Dai, S. Chen and X. C. Xie, Phys. Rev. A **78**, 023603 (2008).
[31] G. B. Jo *et al.*, Science **325**, 1521 (2009).